Available online at www.worldnewsnaturalsciences.com

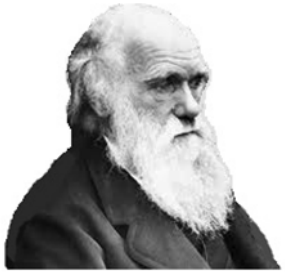

World News of Natural Sciences

WNOFNS 15 (2017) 139-161 EISSN 2543-5426

Optimization of corrosion inhibition of *Picralima nitida* leaves extract as green corrosion inhibitor for zinc in 1.0 M HCl

J. N. O. Ezeugo[1,*], O. D. Onukwuli[2], M. Omotioma[3]

[1]Department of Chemical Engineering, Chukwuemeka Odumegwu Ojukwu University, Anambra State, Nigeria

[2] Department of Chemical Engineering, Nnamdi Azikiwe University, Awka, Nigeria

[3]Department of Chemical Engineering, Enugu State University of Science and Technology, Enugu, Nigeria

*E-mail address: jn.ezeugo@coou.edu.ng

ABSTRACT

Herein, the optimization of inhibitive action of the ethanol extract of oil from *Picralima nitida* leaves, towards acid corrosion of zinc, was tested using weight loss and thermometry methods. We found that the extract acts as a good corrosion inhibitor for zinc corrosion in 0.1 M HCl solutions. The inhibition action of the extract was discussed in view of Langmuir adsorption isotherm. This revealed that spontaneous processes govern the adsorption of the extract on zinc surface. Herein, the inhibition efficiency (*IE*) increases in line with corresponding increase in extract concentration. The temperature effect of the corrosion inhibition on the *IE* was also studied. This indicated that the presence of the extract increases the needed activation energy of the corrosion reaction. Furthermore, in our work, an optimal inhibition efficiency *IE* (%) of 86.78 was obtained at optimum inhibitor concentration of 1.2 $g{\cdot}l^{-1}$, optimum temperature and time of 313 K, and 8 hours, respectively. From the calculated thermodynamic parameters, it can be said, then, that *Picralima nitida* extract provides a good protection to zinc against pitting corrosion in chloride ion containing solutions.

***Keywords*:** Zinc, corrosion, *Picralima nitida*, inhibitor, optimization

(Received 06 November 2017; Accepted 23 November 2017; Date of Publication 24 November 2017)

1. INTRODUCTION

Corrosion is an electrochemical process that gradually returns metals such as zinc to its natural state in the environment. In other words, corrosion can be said to be destruction of material resulting from exposure and interaction with the environment. It is a major problem that requires immediate confrontation for safety, environment, and economic reasons. This ugly menace was also identified by (Thompson *et al*., 2007). Zinc is a component of a wide variety of alloys used since ancient times. Building industry frequently uses zinc alloys in roofing of house and other construction work because of its ductility and malleability. Therefore, zinc alloys are widely used in the production of many components and die-casting fittings in automobile, manufacturing and the mechanical industry, thanks to its good protection or super plasticity.

Zinc, in spite of the so called super plasticity, is not spared by corrosion, especially after prolonged period of exposure in corrosive environment, such as HCl. For these reasons, a lot of efforts have been made using corrosion preventive practices, and the use of green corrosion inhibitors is one of them (Anuradha *et al*., 2007). The use of green inhibitors for the control of corrosion of zinc and alloys which are in contact with aggressive environment is an accepted and growing practice, as confirmed by (Valdez *et al*, 2003; Tayloy, 2007; Khaled *et al*., 2008; Bothi *et al*., 2008). Large numbers of organic compounds are being studied to investigate their corrosion inhibition potential. Relation of these studies shows that organic compounds are not only expensive, but also toxic to living beings.

Plant extracts and organic species have therefore become important as an environmentally acceptable, readily available, and renewable source for a wide range of inhibitors (Rajendran *et al*., 2004; Mesbah *et al*., 2007; Okafor *et al*., 2007). They are the rich sources of ingredients which have very high inhibition efficiency and hence termed “Green Inhibitors” (Lebrini *et al*., 2008; Radijcic *et al*., 2008; Refeay *et al*., 2008). Oguzie *et al*., 2006, experimentally suggested that green corrosion inhibitors are biodegradable and do not contain heavy metals or other toxic compounds. The successful use of naturally occurring substances to inhibit the corrosion of the metals in acidic and alkaline environment have been reported by some research groups (Sharma *et al*., 2009; Mabrouk *et al*., 2011; Eddy *et al*., 2012). Research efforts to find naturally organic substances or biodegradable organic materials to be used as effective corrosion inhibitors of a wide number of metals has been one of the key areas in this research work (Hryniewicz, *et al*., 2016, 2017).

The aim of this study is to optimize the inhibitive properties of *Picralima nitida* leaves extract onto zinc in hydrochloric acid media using a response surface methodology (RSM). Several studies have already been carried out and have remained focused on the *Picralima nitida* leaves extract for their various pharmacological activities. Firstly, *Picralima nitida* plant is a tree that can reach a height of 35 meters, but is usually less. It is a commonly used herbal remedy in the West Africa. All parts of the plant are bitter throughout its distribution area. The seeds, barks, roots, and leaves have a reputation as a febrifuge and remedy for malaria, as well as also being extensively used for pain relief and treatment of chest and stomach problems, pneumonia and intestinal worms (Nagam *et al*., 2012). A decoction of the leave is taken as a treatment for measles. The *Picralima nitida* leave contains many organic compounds, such as phenolics, terpenoids, and tannins as their major phytocompounds, and also saponins, flavonoids, and alkaloids in moderate amount to scavenge free radicals inducing detoxification.

Presently, to the best of our knowledge, no reported work in the area of environment has been carried out on the corrosion inhibitive properties of the *Picralima nitida* leaves extract. Therefore, the aim of this research is to carry out a thorough investigation towards that, in 0.1 M HCl using the leaves extract of the study was done using thermometer, weight loss (Gravimetric) method, and FTIR analysis. The effect of temperature and concentration on the rate of corrosion were also studied, and some thermodynamic and kinetic parameters were calculated, too. Application of central composite design (CCD) for optimization using statistical approaches such as RSM can be employed to maximize independent variable factors (inhibition concentrations, temperature, and time) affecting corrosion inhibition processes in order to secure optimal expected responses, such as weight loss, corrosion rate and inhibition efficiency (E.E. Oguzie, 2006; Mabrouk, E. M. *et al*., 2011)

2. EXPERIMENTAL METHODS

2. 1. Materials

Gravimetric and thermometric tests were performed on 99.988% Zn, other components (wt%) were: Pb 0.003, Cd 0.003, Fe 0.002, Sn 0.001, Cu 0.00, Al 0.001. The sheet of zinc was cut into coupons (2.6 cm × 2.6 cm × 0.015 cm), cleaned and polished with emery paper to expose shining polished surface. The coupons were degreased with acetone in order to remove any trace of oil and impurities, and finally washed with double distilled water, dried in air and then stored in desiccators prior to use.

The aggressive solution 1.0 M HCl was made from analytical grade hydrochloric acid (37%), and distilled water. *Picralima nitida* leaves, collected from Uke in Anambra, Nigeria, were sun-dried for three days. The dried leaves were ground to increase the surface area and stored in a closed container. For every of the extraction process, 30 grams of each of the ground *Picralima nitida* leaves were measured and soaked in 100 ml of ethanol for 48 hours. At the end of the 48 hrs, each plant mixture was filtered. The filtrate is the mixture of the plant extract and the ethanol. The extract of *Picralima nitida* leaves, obtained in ethanol solvent, was concentrated, distilled off the solvent, and evaporated to dryness. The plant extract was weighed and stored for the corrosion inhibition study.

2. 2. Fourier Transform Infrared (FTIR) Analysis of *Picralima nitida* extract and Corrosion Production

The zinc was immersed in the HCl medium in the presence of the *Picralima nitida* leaves extract. At the end of the corrosion study, the corrosion products in the beakers were collected with aid of sample bottles SHIMADZU FT-IR spectrophotometer, model: IR affinity – 1, 5/NA 2137470136 SI), used for the determination of the functional groups of the leaves extract of PNL (pure) and corrosion products in the presence of the PNL extract (Octave, 2003; Nwabunne *et al*., 2011; Nnanna *et al*., 2013; Rubite-Okorosaye, 2004). Comparative analysis of various FTIR produced peaks were carried out in order to determine the exact functional groups for the corrosion inhibition process.

2. 3. Thermometric Method of the Corrosion Inhibition Study

The measurements were carried out using a thermostat set at 30 °C for the zinc in free and inhibited HCl. The temperatures of the system containing the zinc and the test solution were recorded regularly until a steady temperature value was evaluated using eqn. (1) (Deng, 2012; Patel *et al*., 2013; Alino *et al*., 2013; Satapathy *et al*., 2009):

$$RN = \frac{T_m - T_i}{t} \qquad (1)$$

where: T_m and T_i are the maximum and initial temperatures (°C), respectively, and t is the time in minutes elapsed to reach T_m.

The inhibitor efficiency was determined using eq. (2):

$$IE\% = 1 - \frac{RN\ add}{RN\ free} \times 100 \qquad (2)$$

where: RN_{free} and RN_{add} are the reaction numbers for the zinc dissolution in free and inhibited corrosive medium, respectively.

2. 4. Weight loss (gravimetric) method using one factor at a time

The weight loss method was carried out applying one factor at a time. Considering the said method, the weight loss method was carried out at different temperatures and with various concentrations of the *Picralima nitida* extract. Weighed zinc coupons were separately immersed in 250 ml open beakers containing 200 ml of 1.0 M HCl. More so, zinc coupons were separately immersed in 150 ml open beakers containing 200 ml of 1.0 M HCl with various concentrations of PNL extract.

The variation of weight loss was monitored periodically at various temperatures in the absence and presence of various concentrations of the extracts. At the appropriate time, the coupons were taken out, immersed in acetone, scrubbed with a bristle brush under running water, dried and re-weighed. The weight loss was calculated as the difference between the initial weight and the weight after the removal of the corrosion product. The experimental readings were recorded. The weight loss (Δw), corrosion rate (CR) and inhibition efficiency (IE) were determined using the eqns (3), (4), and (5), respectively. The surface coverage was obtained using equation 5 (El-Etre, 2003):

$$\Delta w = wi - wf \qquad (3)$$

$$CR = \frac{we - fe}{At} \qquad (4)$$

$$(IE\%) = \frac{w_0 - w_1}{w_0} \times 100 \qquad (5)$$

$$\theta = \frac{w_0 - w_1}{w_0} \qquad (6)$$

where: w_i and w_f are the initial and final weight of zinc samples, respectively, W_1 and W_0 are the weight loss values in the presence and absence of inhibitor, respectively; A is the total area of the zinc sample and t is the immersion time.

2. 5. Effect of Temperature on the Corrosion Rate

Effect of temperature on the corrosion rate was described using Arrhenius equation:

$$CR = A\, e^{-Ea/RT} \qquad (7)$$

where: CR is the corrosion rate of the zinc, A is the pre-exponential factor, Ea is the activation energy, R is the universal gas constant. Equation (7) can be linearized to form eq. (8):

$$In\,(CR) = In\,A - \left({}^{Ea}/_{R}\right)\left(\frac{1}{T}\right) \qquad (8)$$

Considering the corrosion rate of the zinc at T_1 and T_2 as CR_1 and CR_2, then eq. (8) can be expressed by eq. (9) [18, 20]. As follows:

$$In\left(\frac{CR_2}{CR_1}\right) = \left(\frac{Ea}{2.303R}\right)\left(\frac{1}{T_1} - \frac{1}{T_2}\right) \qquad (9)$$

Thermodynamic parameter for the adsorption process; The heat of adsorption Q_{ads} (kJ·mol^{-1}) was calculated using eq. (10) [21]:

$$Qads = 2.303R\left[\log\left(\frac{\theta_2}{1-\theta_2}\right) - log\left(\frac{\theta_1}{1-\theta_1}\right) \times \frac{T_2\,T_1}{T_2 - T_1}\right] \qquad (10)$$

where: R is the gas constant, θ_1 and θ_2 are the degrees of surface coverage at temperature T_1 and T_2, respectively.

2. 6. Consideration of the adsorption isotherm

The data obtained for the degree of surface coverage were used to test for the applicability of different adsorption isotherms (Langmuir, Frumkin, Temkin, and Flory-Huggins isotherms).

1) Langmuir Isotherm

Langmuir isotherm can be expressed by eq. (11) (Umoren and Ebenso, 2007).

$$\frac{C}{\theta} = \frac{1}{K} + C \qquad (11)$$

where: C is the concentration of the inhibitor, K is the adsorption equilibrium constant and θ is the degree of surface coverage. In logarithmic form, eq. (11) can be expressed in eq. (12):

$$\log\frac{C}{\theta} = \log C - \log K \qquad (12)$$

2) Frumkin Isotherm

Frumkin adsorption isotherm can be expressed according to eq. (13):

$$\log\left(Cc) * \left(\frac{\theta}{1-\theta}\right)\right) = 2.303logK + 2\,\alpha\theta \qquad (13)$$

where: K is the adsorption – desorption constant, and α is the lateral interaction term describing the interaction in adsorbed layer.

3) Temkin isotherm

Temkin isotherm can be expressed by eq. (14) [19]:

$$\theta = \frac{2.303\log K}{2a} - \frac{2.303\log C}{2a} \qquad (14)$$

where: K is the adsorption equilibrium constant, a is the attractive parameter, θ is the degree of surface coverage, and C is the concentration of the inhibitor.

4) Florry-Huggins Isotherm

The Flory-Huggins isotherm can be expressed by eq. (15):

$$\log\left(\frac{\theta}{C}\right) = \log K + x\log(1-\theta) \qquad (15)$$

where: x is the size parameter and is a measure of the number of adsorbed water molecules. The free energy of adsorption (ΔG_{ads}) was calculated according to eq. (16) (Khadom *et al*., 2009; Cabot *et al*., 1991):

$$\Delta G_{ads} = -2.303RT\log(55.5K) \qquad (16)$$

where: R is the gas constant, T is the temperature, K values obtained from the isotherms (Langmuir, Frumkin, Temkin, and Flory-Huggins isotherms) were used to obtain the values of ΔG_{ads} according to eq. (16).

3. RESULTS AND DISCUSSION

3. 1. FTIR Spectrophotometer

FTIR Spectrophotometer is a strong instrument that can be used to identify the type of bonding, especially functional group (s) present in the organic compounds. **Fig. 1** shows the *IR* spectrum of the ethanolic extract of *Picralima nitida* leaves extract. Initial absorption at 3952.4 to 3543.24 cm^{-1} (associated hydroxyl) was overlapped by the strong stretching bond of O-H.

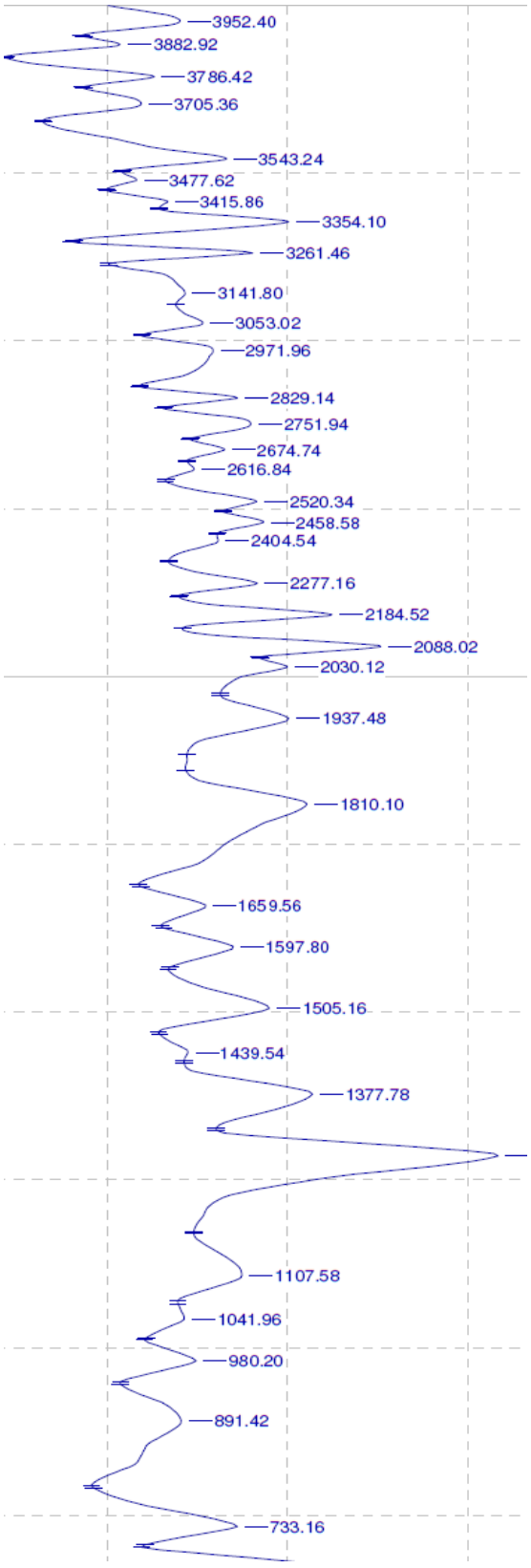
3952.40
3882.92
3786.42
3705.36
3543.24
3477.62
3415.86
3354.10
3261.46
3141.80
3053.02
2971.96
2829.14
2751.94
2674.74
2616.84
2520.34
2458.58
2404.54
2277.16
2184.52
2088.02
2030.12
1937.48
1810.10
1659.56
1597.80
1505.16
1439.54
1377.78
1107.58
1041.96
980.20
891.42
733.16

(a)

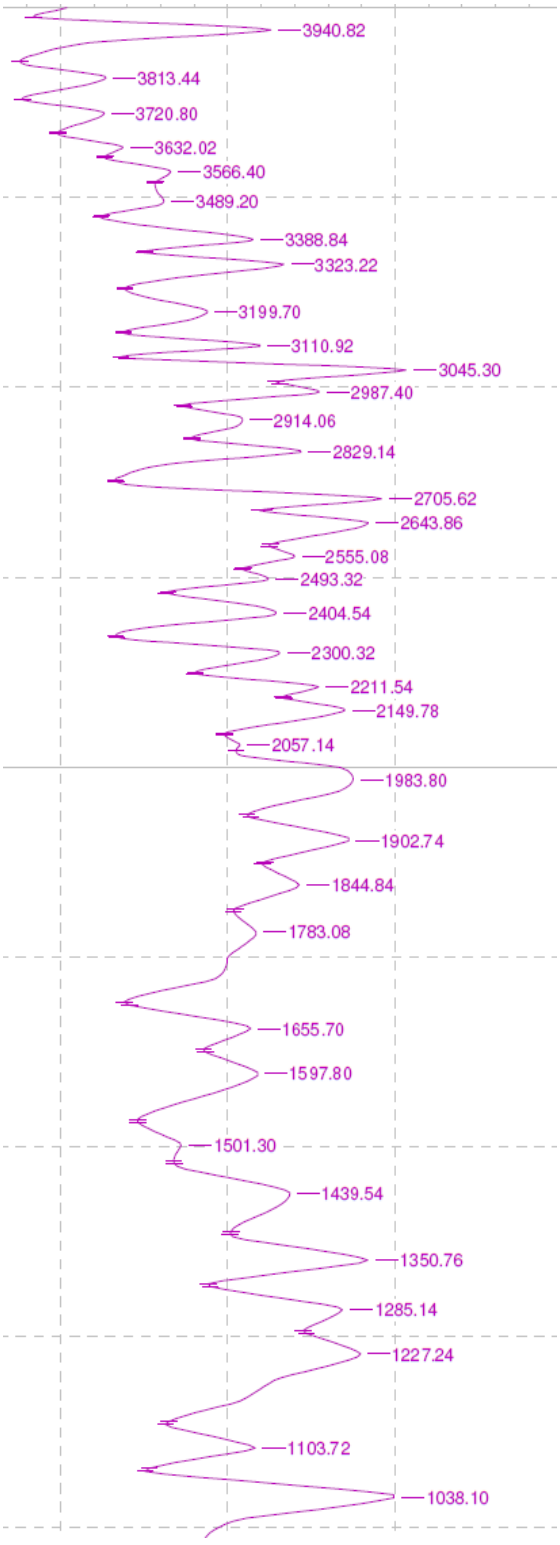

(b)

Fig. 1. FTIR spectrum of **(a)** pure extract of *Picralima nitida* leave **(b)** corrosion product of zinc in HCl medium with *Picralima nitida* extract.

The peaks at 3477.62 to 3261.46 cm^{-1} are attributed to the medium and often broad stretch band of amines and amides, N-H. Wave bands 3141.8 and 3053.02 cm^{-1} are variable stretch of alkyl and aldehyde bond group, C-H. The absorption band at 2971.96 cm^{-1} stands for strong and very broad stretch of carboxylic acid (free bond of alcohol). Wave band of 2751.94 cm^{-1}, 2829.14 cm^{-1} are two-peaked medium stretch bond of aldehyde, C ≡ C. The peak at 2404.54 to 2030.12 cm^{-1} represents variable and sharp stretch bond of alkyne and nitrite, C=N. Wave bands 1837.48 cm^{-1}, 1658.65 cm^{-1} are strong representatives of stretch bond of acids, esters, anhydrides, and aldehydes, C=O. The absorption bands 1597.8 cm^{-1}, 1439.54 cm^{-1} are multiple sharp, medium peaks stretch of aromatic bond, C=C. This shows that *Picralima nitida* leaves extract contains mixtures of compounds, that is, alkaloids, flavonoids, phenolics, phytates, terpenoids, tannins, and steroids (Satapathy *et al*., 2009).

3. 2. Results of the Corrosion Inhibition as Determined by Thermometric Studies

The effect of concentration of *Picralima nitida* leaves (inhibitor) extract on the reaction number (*RN*) and the inhibition efficiency (*IE*) of zinc in the 0.1 M HCl medium is presented in **Table 1**. It was revealed that increase in concentration of the inhibitor lowers the reaction number. This is in agreement with a previous observation (Librini *et al*., 2008). More so, the inhibition efficiency increases with increasing concentration of the inhibitor.

Table 1. Effect of the *Picralima nitida* leaves extract on the *IE*(%) of zinc in 0.1 M HCl medium

Inhibitor concentration (gL^{-1})	*RN*	*IE* (%)
0	0.1714	
0.2	0.0863	49.65
0.45	0.0686	59.98
0.7	0.0423	75.33
0.95	0.033	80.74
1.2	0.027	84.25

3. 3. Weight loss measurement

Fig. 2 represents the relation between time and inhibition efficiency of zinc in 0.1 M HCl at various concentrations of *Picralima nitida* leaves extract, while **Table 2** represents experimental results of the weight loss and corrosion rate using one factor at a time.

Inspection of Fig. 2 reveals that the loss of weight increases linearly with increasing time in all tested solutions. However, the slopes of the obtained lines which represent the rate of weight loss, are affected by the addition of *Picralima nitida* extract. The presence of the extract

causes a sharp decrease in the rate of weight loss. *IE*s at different concentrations of the extract were calculated using the equation (17):

$$IE(\%) = \frac{w_0 - w_1}{w_0} \times 100 \qquad (17)$$

where: W_1 and W_0 are the weight loss values in the presence and absence of inhibitor, respectively.

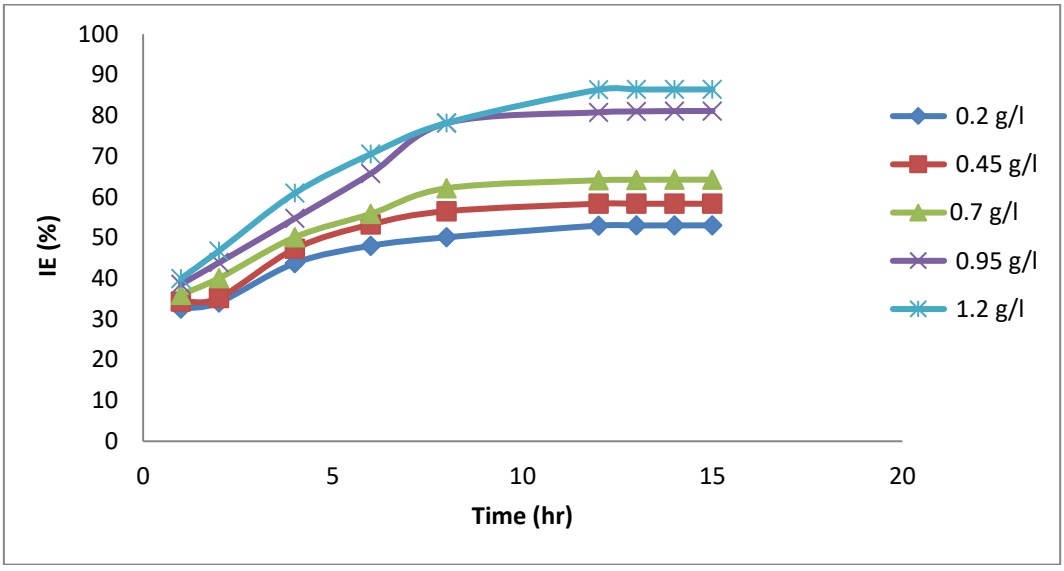

Fig. 2. Plot of *IE*(%) of zinc in HCl versus time at various concentrations of PNL extract.

Table 2. Corrosion inhibition of zinc in 0.1 M HCl with *Picralima nitida* leaves extract

Time (h)	Temperature (K)	Inhibitor conc. ($g \cdot L^{-1}$)	Weight loss (g)	Corrosion rate ($mg/cm^2 \cdot h$)	Inhibition efficiency (%)	Degree of surf. cov.
12	303	0	0.521	4.824	-	-
		0.2	0.245	2.269	52.98	0.5298
		0.45	0.217	2.009	58.35	0.5835
		0.7	0.187	1.731	64.11	0.6411
		0.95	0.1	0.926	80.81	0.8081
		1.2	0.071	0.657	86.37	0.8637
12	313	0	0.545	5.046	-	-
		0.2	0.323	2.991	40.73	0.4073
		0.45	0.264	2.444	51.56	0.5156
		0.7	0.19	1.759	65.14	0.6514
		0.95	0.145	1.343	73.39	0.7339
		1.2	0.117	1.083	78.53	0.7853

12	323	0	0.61	5.648	-	-
		0.2	0.391	3.62	35.9	0.359
		0.45	0.31	2.87	49.18	0.4918
		0.7	0.23	2.13	62.3	0.623
		0.95	0.175	1.62	71.31	0.713
		1.2	0.172	1.593	71.8	0.718

The values of *IE*s and θs different *Picralima nitida* extract concentrations are given in **Table 2**. The tabulated data revealed that, the *Picralima nitida* leave extract acts as a good corrosion inhibitor for the acid corrosion of zinc. The corrosion inhibition increases with increasing extract concentration. The analysis of the *Picralima nitida* extract revealed that the ethanolic extract contains toluene, formular, C_7H_8, molecular weight, 92, cyclohexane having formula C_8H_{16}, molecular weight 112, hexane, 1,3-cyclopenta deine, molecular weight, 156. It also contains at least ten non-volatile acids including eicosane and citric acids. The adsorption of the compounds on the electrode surface makes a barrier for mass and charge transfers, as confirmed by (El-Etre, 2003). The outcome of this situation leads to a protection of the metal surface from the attack of the aggressive anions of the acid. The extent of protection increases with increasing of the surface fraction occupied by the adsorbed molecules. As the extract concentration is increased, the number of the adsorbed molecules on the surface increases. **Table 2** represents also the values of adsorption isotherm parameter. From the Table, a parameter (θ), which was estimated from the *IE* values, could be used to represent the fraction of the surface occupied by the adsorbed molecules. Inept examination of Table 2 reveals that the values of θ increase with increasing inhibitor concentrations. The dependence of the fraction of the surface occupied by the adsorbed molecules on the inhibitor concentration (c) is shown in **Fig. 3**. A plot of C/θ versus C gives a straight line with a unit slope. The results indicate that the adsorption of inhibitor molecules on the zinc surface follows Langmuir isotherm. In other words, the result suggests that there are no interactions or repulsion forces between the adsorbed molecules. It is of interest to note here that, the θ values obtained from the other used techniques also obey the Langmuir adsorption isotherm.

The standard adsorption free energy (ΔG_{ads}) was calculated using the following equation (Umoren and Ebenso, 2007):

$$K = \frac{1}{999}\exp\left(-\frac{\Delta G_{ads}}{RT}\right) \qquad (18)$$

where 999 is the concentration of water in solution expressed in $g \cdot L^{-1}$. R is gas constant, and T - absolute temperature. The mean values of standard adsorption free energy (ΔG_{ads}) was –46.4018 $kJ \cdot mol^{-1}$. The negative value of ΔG_{ads} guarantees the spontaneity of the adsorption process and stability of the adsorbed layer on the metal surface. It is generally known that, the values of ΔG_{ads} up to –20 $kJ \cdot mol^{-1}$ is consistent with electrostatic interaction between the charged molecules and the charged metal (physisorption) while those around –40 $kJ \cdot mol^{-1}$ or higher are associated with chemisorptions, as a result of sharing or transfer of electrons from the molecules to the metal surface to form a coordinate type of bond. Other researchers, however, suggested that the range of ΔG_{ads} of chemical adsorption processes for inhibitor in

aqueous media lies between –21 and –42 kJ·mol^{-1}. Similar results were gotten by (Umoren and Ebenso, 2007; Khadom *et al*., 2009).

Table 3. Adsorption parameters for the corrosion inhibition of zinc in HCl by PNL extract

Adsorption isotherm	Temperature (K)	R^2	Log K	K	ΔGads (kJ·mol^{-1})	Isotherm property	
Langmuir isotherm	303	0.992	–0.155	0.6998	–9.220		
	323	0.978	–0.108	0.7834	–10.132		
Frumkin isotherm	303	0.967	–1.1772	0.0665	–3.290	α	2.086
	323	0.993	–0.9917	0.1019	–4.653		1.899
Temkin isotherm	303	0.834	–1.8252	0.0150	0.461	a	–2.684
	323	0.976	–1.3992	0.0399	–2.135		–2.321
Flory-Huggins isotherm	303	0.622	0.474	2.9785	–12.869	x	0.762
	323	0.926	0.427	2.6730	–13.428		1.119

From **Table 3**, the values of ΔG_{ads}, as recorded in the present work, has been considered within the range of physical adsorption. Limited increase in the absolute value of ΔG_{ads} at 303 K temperature, then, heat of adsorption decreases again at 313 K, indicating that the adsorption was somewhat favorable at the experimental temperature, and *Picralima nitida* leaves extract adsorbed according to physical mechanisms, i.e. desorption of inhibitor molecules when temperature increased.

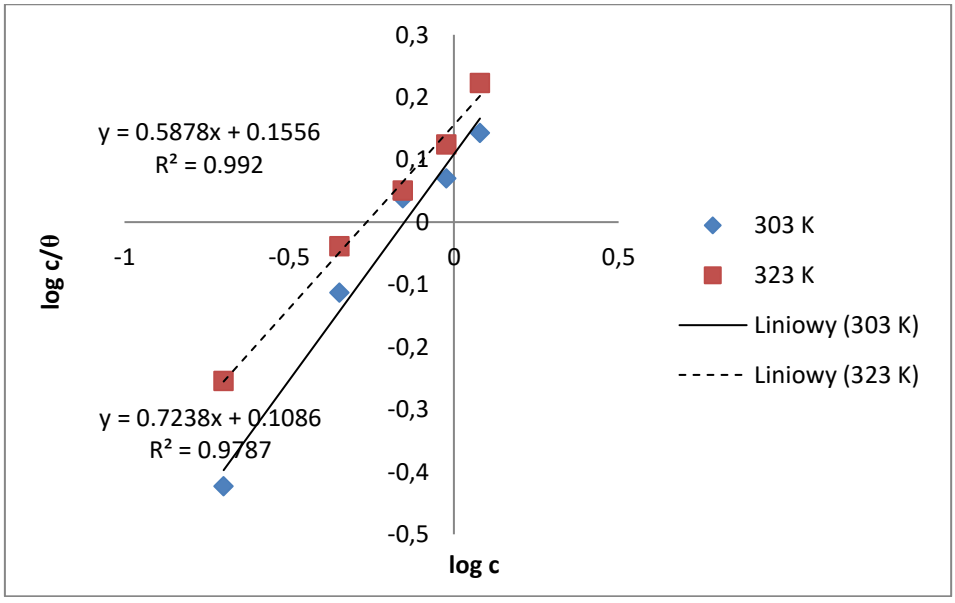

Fig. 3. Plots of Langmuir isotherm for zinc in HCl with PNL extract.

Moreover, the major characteristic Langmuir isotherm can be expressed in terms of linear regression coefficient. The value of the linear regression coefficient is close to unity, hence, adsorption of the *Picralima tinida* leaves extract follows Langmuir isotherm and R^2 value is $0.994 \geq 0.982$. It is very important to note that the smaller values of R^2 indicate a highly favorable adsorption. $R^2 > 1$ unfavorable, $R^2 = 1$ linear, $0 < R^2 < 1$ favorable and if $R^2 = 0$, irreversible. Table 3 shows the various values of R^2 for the entire tested isotherms model. The values of K_{ads} are relatively small, indicating that the interaction between the adsorbed extract molecules and metal surface is physically adsorbed.

A close look at **Table 4** shows various inhibition concentrations ($g \cdot L^{-1}$) and their respective activation energy ($kJ \cdot mol^{-1}$). From the Table, calculated *E*a values for the inhibited solution with *Picralima nitida* extract are 52.404 and 82.985 $kJ \cdot mol^{-1}$ in the presence of the inhibitor of 0.95 and 1.2 $g \cdot L^{-1}$ extract concentrations, while with 0.45 and 0.70 $g \cdot L^{-1}$ concentration, the activation energies are 33.418 and 19.434 $kJ \cdot mol^{-1}$. The higher values of *E*a suggest that dissolution of zinc in the presence of inhibitor is slow, indicating a strong inhibitive action of phytocompounds of alkaloids, flavonoids and tannins presence in *Picralima nitida* leaves extracts, which leads to increasing the energy barrier for the corrosion process (Cobot *et al*., 1991). Actually, toluene molecules (the main compound of *Picralima nitida* leave extracts oil) are easily protonated and exist in 0.1 M HCl medium in cationic form. Indeed, it is logical to assume that in this study, the electrostatic cation adsorption is responsible for the good protective properties of this compound.

Table 4. Activation Energy and Heat of Adsorption for the Corrosion Inhibitor of Zinc in 0.1 M HCl at various Inhibition Concentrations

Inhibitor concentration ($g \cdot L^{-1}$)	*E*a ($kJ \cdot mol^{-1}$)	ΔG_{ads} ($kJ \cdot mol^{-1}$)
0.2	43.768	–28.445
0.45	33.418	–15.054
0.7	19.434	–3.167
0.95	52.404	–21.453
1.2	82.985	–37.102

3. 4. Results of the gravimetric method using RSM approach

The expected responses of weight loss, corrosion rate, and inhibition efficiency to the independent variables, such as concentration, temperature, and time in respect to corrosion inhibition of *Picralima nitida* leave extracts, as a green corrosion inhibitor for zinc in HCl, are listed in **Table 5**.

3. 5. Graphical Analysis of the Inhibition Efficiency, *IE* (%), as determined using (RSM)

Response surface methodology (RSM) was used to analyze the response. The ANOVA and graphical analyses of the inhibition efficiencies were carried out. The mathematical models in terms of coded and actual factors were obtained. The model in terms of coded factors was used to make predictions about the response for the given levels of each factor.

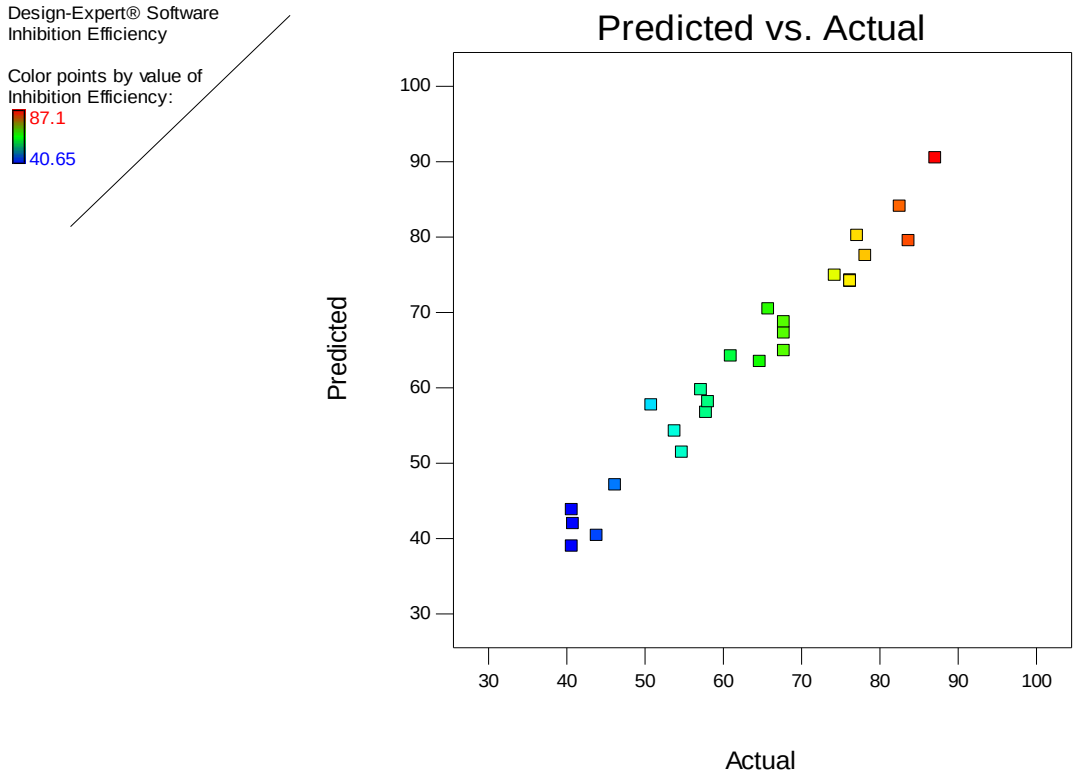
Design-Expert® Software
Inhibition Efficiency
Color points by value of
Inhibition Efficiency:
87.1
40.65
Predicted vs. Actual
Predicted
Actual
100
90
80
70
60
50
40
30
30
40
50
60
70
80
90
100

(a)

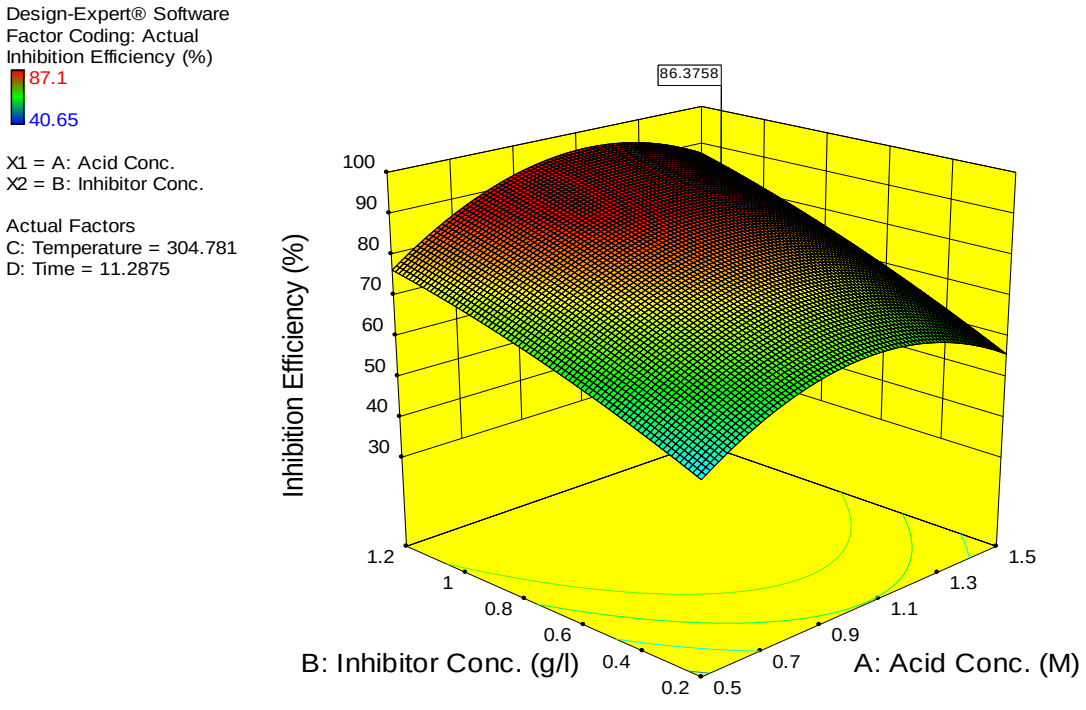
Design-Expert® Software
Factor Coding: Actual
Inhibition Efficiency (%)
87.1
40.65
X1 = A: Acid Conc.
X2 = B: Inhibitor Conc.
Actual Factors
C: Temperature = 304.781
D: Time = 11.2875
86.3758
Inhibition Efficiency (%)
100
90
80
70
60
50
40
30
B: Inhibitor Conc. (g/l)
1.2
1
0.8
0.6
0.4
0.2
A: Acid Conc. (M)
0.5
0.7
0.9
1.1
1.3
1.5

(b)

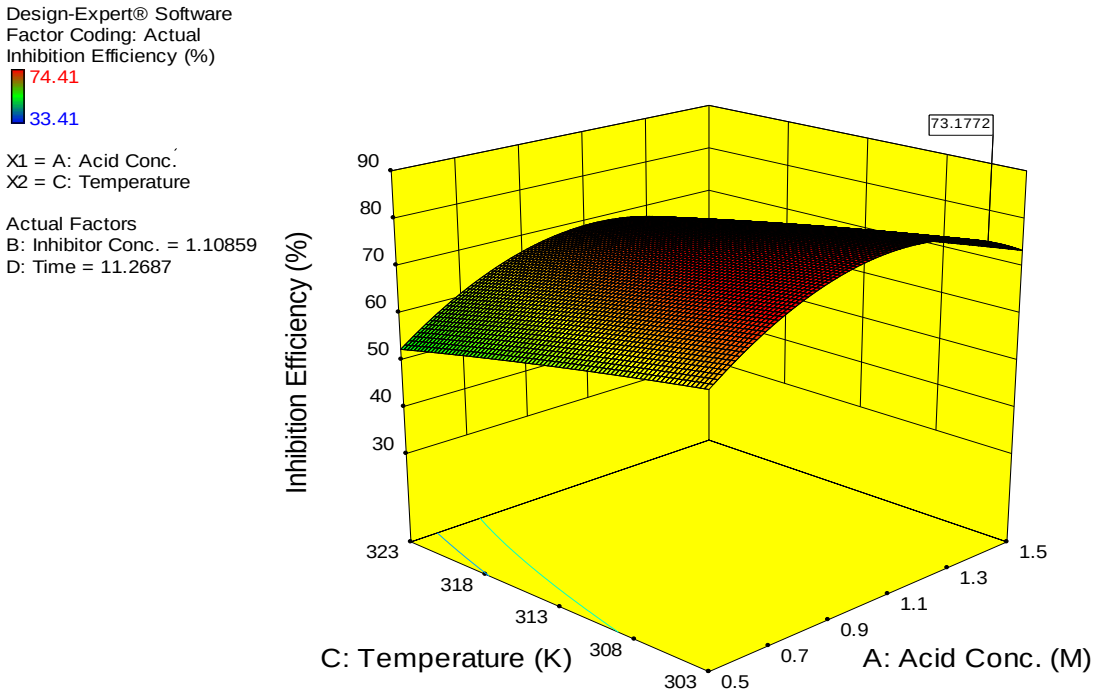
Design-Expert® Software
Factor Coding: Actual
Inhibition Efficiency (%)
74.41
33.41
X1 = A: Acid Conc.
X2 = C: Temperature
Actual Factors
B: Inhibitor Conc. = 1.10859
D: Time = 11.2687
73.1772
Inhibition Efficiency (%)
90
80
70
60
50
40
30
323
318
313
308
303
C: Temperature (K)
0.5
0.7
0.9
1.1
1.3
1.5
A: Acid Conc. (M)

(c)

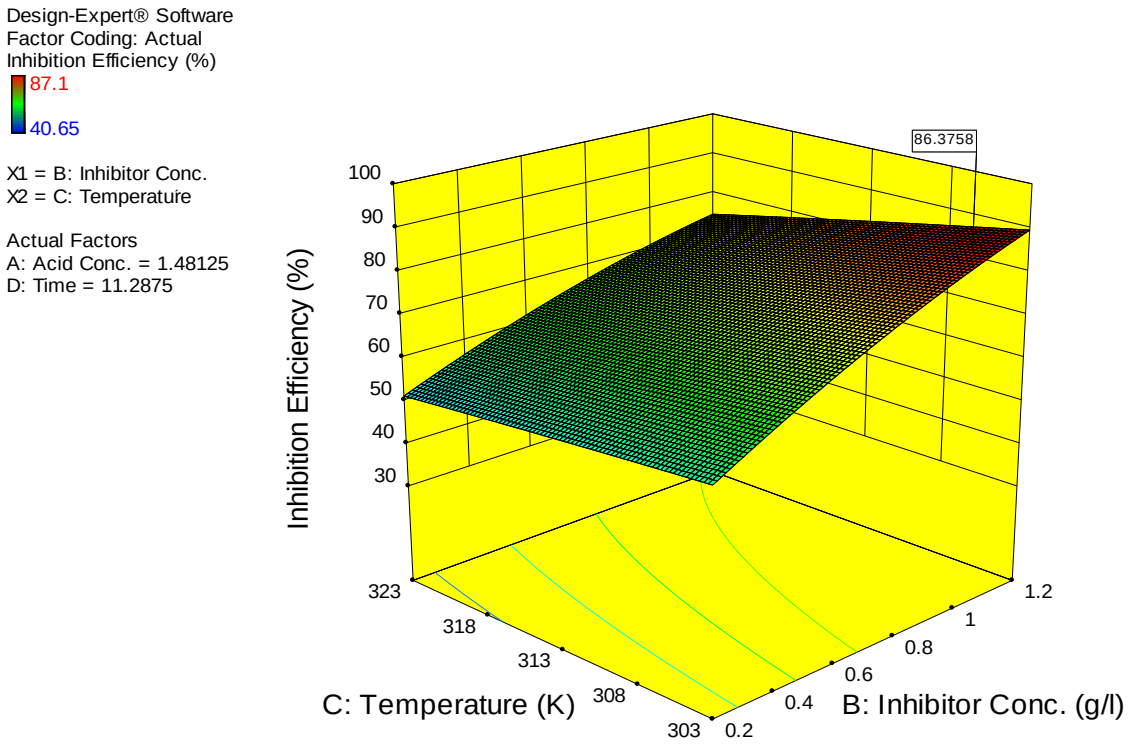
Design-Expert® Software
Factor Coding: Actual
Inhibition Efficiency (%)
87.1
40.65
X1 = B: Inhibitor Conc.
X2 = C: Temperature
Actual Factors
A: Acid Conc. = 1.48125
D: Time = 11.2875
86.3758
Inhibition Efficiency (%)
100
90
80
70
60
50
40
30
323
318
313
308
303
C: Temperature (K)
0.2
0.4
0.6
0.8
1
1.2
B: Inhibitor Conc. (g/l)

(d)

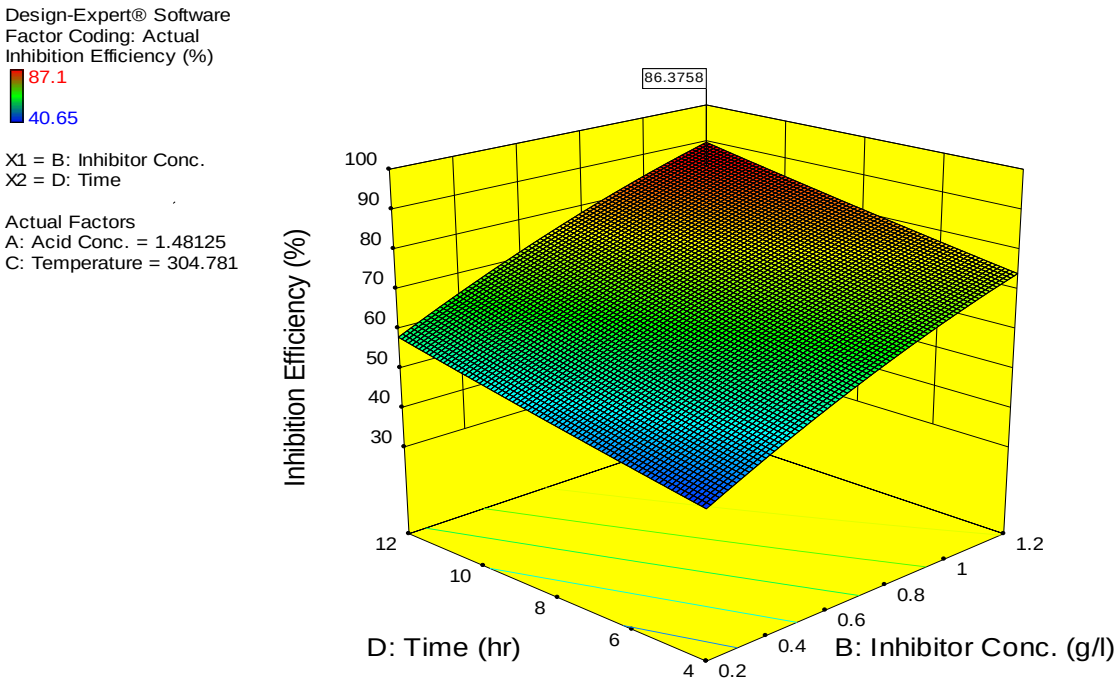
Design-Expert® Software
Factor Coding: Actual
Inhibition Efficiency (%)
87.1
40.65
X1 = B: Inhibitor Conc.
X2 = D: Time
Actual Factors
A: Acid Conc. = 1.48125
C: Temperature = 304.781
86.3758
Inhibition Efficiency (%)
100
90
80
70
60
50
40
30
12
10
8
6
4
D: Time (hr)
0.2
0.4
0.6
0.8
1
1.2
B: Inhibitor Conc. (g/l)

(e)

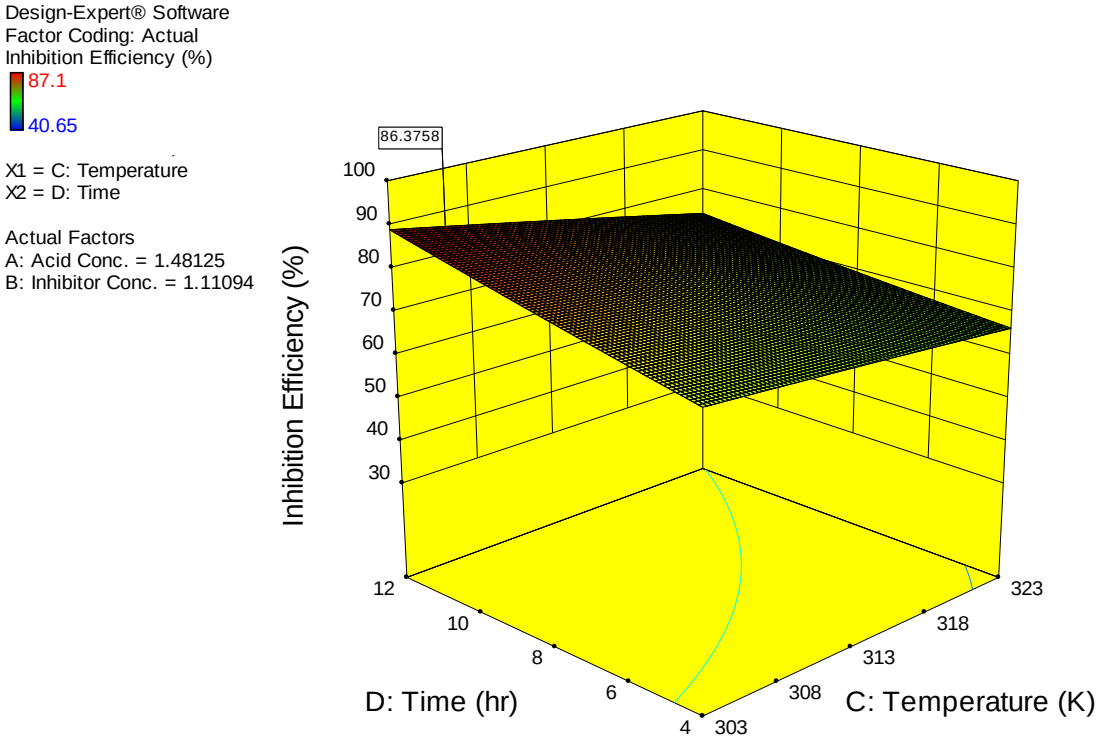
Design-Expert® Software
Factor Coding: Actual
Inhibition Efficiency (%)
87.1
40.65
X1 = C: Temperature
X2 = D: Time
Actual Factors
A: Acid Conc. = 1.48125
B: Inhibitor Conc. = 1.11094
86.3758
Inhibition Efficiency (%)
100
90
80
70
60
50
40
30
12
10
8
6
4
D: Time (hr)
303
308
313
318
323
C: Temperature (K)

(f)

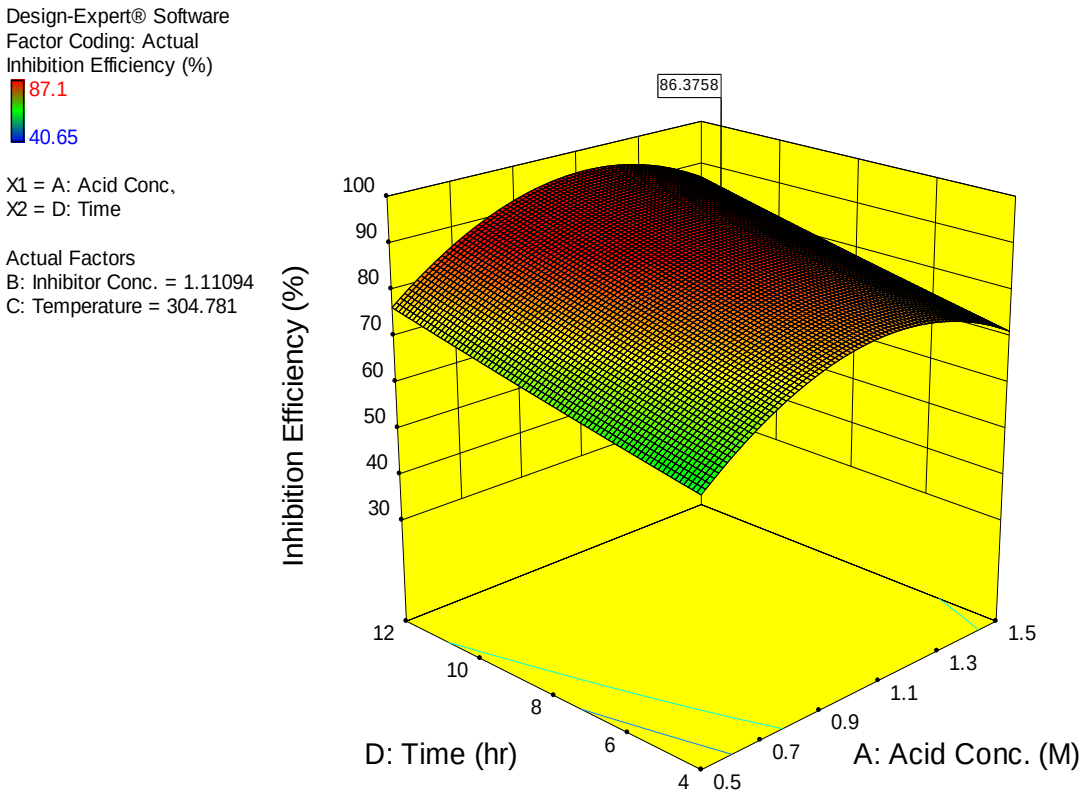

(g)

Figure 4. *IE* (%) of Zn in HCl Medium with PNL Extract

Table 5. RSM Result of the Inhibition of Zn in HCl Medium with PNL Extract

Std	Run	Factor 1, A. Acid Conc. (M)	Factor 2 B. Inhibitor Conc. (g/L)	Factor 3, C. Temperature (K)	Factor 4, D. Time (h)	Response 1, Weight Loss (g)	Response 2, Corrosion Rate (mg/cm^{2}h)	Response 3, Inhibition Efficiency (%)
23	1	1	0.7	313	4	0.109	3.025	67.75
21	2	1	0.7	303	8	0.082	1.134	78.16
13	3	0.5	0.2	323	12	0.327	3.025	46.19
27	4	1	0.7	313	8	0.109	1.512	76.21
29	5	1	0.7	313	8	0.109	1.512	76.21
7	6	0.5	1.2	323	4	0.163	4.537	57.81
4	7	1.5	1.2	303	4	0.082	2.269	76.21
6	8	1.5	0.2	323	4	0.245	6.806	40.65

3	9	0.5	1.2	303	4	0.109	3.025	60.97
30	10	1	0.7	313	8	0.109	1.512	76.21
22	11	1	0.7	323	8	0.163	2.269	65.76
9	12	0.5	0.2	303	12	0.218	2.017	53.8
14	13	1.5	0.2	323	12	0.327	3.025	54.72
10	14	1.5	0.2	303	12	0.245	2.269	58.06
19	15	1	0.2	313	8	0.191	2.647	57.16
1	16	0.5	0.2	303	4	0.163	4.537	40.65
16	17	1.5	1.2	323	12	0.191	1.764	74.26
11	18	0.5	1.2	303	12	0.082	0.756	83.68
24	19	1	0.7	313	12	0.163	1.512	77.11
2	20	1.5	0.2	303	4	0.163	4.537	40.81
25	21	1	0.7	313	8	0.109	1.512	76.21
20	22	1	1.2	313	8	0.082	1.134	82.56
26	23	1	0.7	313	8	0.109	1.512	76.21
17	24	0.5	0.7	313	8	0.191	2.647	50.81
8	25	1.5	1.2	323	4	0.136	3.781	67.75
15	26	0.5	1.2	323	12	0.218	2.017	64.67
12	27	1.5	1.2	303	12	0.082	0.756	87.1
18	28	1.5	0.7	313	8	0.163	2.269	67.75
5	29	0.5	0.2	323	4	0.218	6.05	43.84
28	30	1	0.7	313	8	0.109	1.512	76.21

The high levels of the factors were coded as +1 and the low levels of the factors were coded as −1. The optimum inhibition parameters were obtained.

From the RSM graph predicted versus actual plot is used to testy the significance of the model's order. The predicted versus actual plot shows linear graph. The graphs (3-D surface plots) show the relationship between the factors and response (inhibition efficiency) of the designed experiment. Increase in concentration increases the inhibition efficiency. Also inhibition efficiency reduces as temperature rises (**Figure 4**).

Predicted versus actual *IE* (%) (b) *IE* (%) versus inhibition concentration and acid concentration (c) *IE* (%) versus time and acid concentration (d) *IE* (%) versus temperature and acid concentration (e) *IE* (%) versus time and inhibitor concentration (f) *IE* (%) versus time and temperature (g) *IE* (%) versus time and acid concentration.

3. 6. Mathematical models of the inhibition efficiency

The equation in terms of coded factors can be used to make predictions about the response for given levels of each factor. By default, the high levels of the factors are coded as +1 and the low levels of the factors are coded as −1.

The coded equation is useful for identifying the relative impact of the factors by comparing the factor coefficients. The Model F-value of 28.13 implies the model is significant. There is only a 0.01% chance that an F-value this large could occur due to noise. Values of "Prob > F" less than 0.0500 indicate model terms are significant. In this case A, B, C, D, BC, CD, A^2 are significant model terms. Values greater than 0.1000 indicate the model terms are not significant. If there are many insignificant model terms (not counting those required to support hierarchy), the model reduction may improve your model. The "Pred R-Squared" of 0.8010 is in a reasonable agreement with the "Adj R-Squared" of 0.9291; i.e. the difference is less than 0.2."Adeq Precision" measures the signal-to-noise ratio. A ratio greater than 4 is desirable. Your ratio of 19.623 indicates an adequate signal. This model can be used to navigate the design space.

Final Equation in Terms of Coded Factors:

Inhibition Efficiency = +74.17+3.60* A+12.17* B–3.54* C+5.73* D+1.78* AB+0.11* AC+0.23* AD–2.22* BC+9.375E-003* BD–2.14* CD–12.85* A^2–2.27* B^2–0.17* C^2+0.30* D^2….(19)

Final Equation in Terms of Actual Factors:

Inhibition Efficiency = –286.46491 + 97.08940* Acid Conc. + 168.98352* Inhibitor Conc. +1.40306* Temperature+17.74244* Time +7.10750* Acid Conc. * Inhibitor Conc. +0.022375* Acid Conc. * Temperature +0.11406* Acid Conc. * Time -0.44437* Inhibitor Conc. * Temperature +4.68750E-003* Inhibitor Conc. * Time -0.053453* Temperature * Time –51.38526* Acid $Conc.^2$ –9.06526* Inhibitor $Conc.^2$ –1.66316E-003* $Temperature^2$ +0.018980* $Time^2$…..(20)

Table 6. ANOVA Response for inhibition efficiency of Zinc in HCl medium with *Picralima nitida* leaf extract

ANOVA for Response Surface Quadratic model						
Analysis of variance table [Partial sum of squares - Type III]						
	Sum of		**Mean**	**F**	**p-value**	
Source	**Squares**	**df**	**Square**	**Value**	**Prob > F**	
Model	5429.16	14	387.80	28.13	< 0.0001	Significant
A-Acid Conc.	233.93	1	233.93	16.97	0.0009	
B-Inhibitor Conc.	2667.66	1	2667.66	193.54	< 0.0001	
C-Temperature	226.06	1	226.06	16.40	0.0010	
D-Time	591.11	1	591.11	42.89	< 0.0001	

AB	50.52	1	50.52	3.66	0.0748
AC	0.20	1	0.20	0.015	0.9057
AD	0.83	1	0.83	0.060	0.8092
BC	78.99	1	78.99	5.73	0.0302
BD	1.406E-003	1	1.406E-003	1.020E-004	0.9921
CD	73.15	1	73.15	5.31	0.0360
A^2	427.57	1	427.57	31.02	< 0.0001
B^2	13.31	1	13.31	0.97	0.3414
C^2	0.072	1	0.072	5.199E-003	0.9435
D^2	0.24	1	0.24	0.017	0.8970
Residual	206.75	15	13.78		
Lack of Fit	206.75	10	20.68		
Pure Error	0.000	5	0.000		
Cor Total	5635.91	29			

Std. Dev.	3.71	R-Squared	0.9633
Mean	65.18	Adj R-Squared	0.9291
C.V. %	5.70	Pred R-Squared	0.8010
PRESS	1121.36	Adeq Precision	19.623
-2 Log Likelihood	143.05	BIC	194.06
		AICc	207.33

3. 7. Results of the optimum inhibition efficiency

To confirm the validity of the results, additional experiments were conducted. The chosen condition for the concentration, temperature, and time are listed in Table 5, along with the predicted and measured inhibited efficiencies. As shown in **Table 7**, the measured inhibition efficiencies were close to the predicted values. It shows that RSM approach was appropriate for optimizing the corrosion inhibition process.

Table 7. Validation of Result for Corrosion Inhibition of Zn in HCl by Plant Extract

S/N	Inhibitor	Acid Conc. A	Inhibitor Conc. B, (g/L)	Temperature C, (K)	Time D, (h)	Predicted *IE* (%)	Experimental *IE* (%)	Percentage error (%)
1	PNL	1.48	1.11	304.78	11.29	86.38	87.1	0.01

4. CONCLUSIONS

i. The *Picralima nitida* leaves extract acts as a good inhibitor for corrosion of zinc in 0.1 M HCl solution. The *IE* increases with increasing the extract concentration.

ii. The inhibitory action of the extract was carried out through adsorption of the extract compounds on zinc surface. The adsorption process is spontaneous, stable, and obeys Langmuir adsorption isotherm.

iii. The adsorption process is physical as various studies technique points towards physisorption. More so, the increase in temperature decreases the *IE* of the extract.

iv. The presence of *Picralima nitida* extract increases the activation energy of the corrosion reaction.

v. The *Picralima nitida* leaves extract provides a strong protection against corrosion of zinc in the presence of chloride ions. The extent of protection increases with increasing extract concentration and the leave extracts exhibit optimal inhibition efficiency *IE* (%) of 87.56, at optimal inhibition concentration of 1.2 $g \cdot L^{-1}$, temperature and time of 313 K and 8 hours, respectively.

References

[1] I. Radojčić, K. Berković, S. Kovač, J. Vorkapić-Furač, *Corrosion Science* 50 (2008) 1498-1504. https://doi.org/10.1016/j.corsci.2008.01.013

[2] Khadom, A.A. Yaro, A.S. Altaie, A.A.H. Kadum, *Portug. Electrochim. Acta* 27 (6) (2009) 699-712

[3] A.K. Satapathy, G. Gunasekaran, S.C. Sahoo, K. Amit, P.V. Rodrigues, *Corrosion Science* 51 (2009) 2848-2856

[4] A.Y. El-Etre, *Corrosion Science* 45 (2003) 2485-2495

[5] B. Valdez, J. Cheng, F. Flores, M. Schorr, L. Veleva. *Corrosion Rev.* 21 (2003) 445-458

[6] E.E. Oguzie, Pigment. Resin. Tech. 35 (2006) 334-340

[7] E.M. Mabrouk, H. Shoky, K.M. Abu Al-Naja, *Chem. Met. Alloys* 4 (2011) 98-106

[8] I.J. Alinno, P.M. Ejikeme, *America Chem. Sci. J.* 2 (2012) 122-135

[9] J. Anuradha, R. Vimala, B. Narayanasanly, S. Arochia, D.S. Rajendran, *Lenn. Chem. Eng. Comm.* 195 (2008) 352-366.

[10] J.T. Nwabanne, V.N. Okafor, *J. Emer. Trends. In Engin. And App. Sci*. 2 (2011) 619-625

[11] K.F. Khaled. *Int. J. Electrochem. Sci.* 3 (2008) 462-475

[12] K.O. Rubite-Okorosaye, N.C. Oforka, *J. Appl. Sci. Environ. Mgt.* 8 (2004) 57-61

[13] L. Octave, Chemical Reaction Engineering, 3rd eds. John Wily and Sons, New York, 2003.

[14] L.A. Nnanna, I.O. Owate, O.C. Nwadiuko, N.D., Ekekowe, W.J. Oji, *Int. J. Mater. Chem*. 3 (2013) 10-16

[15] M. Lebrini, M. Traisnel, M. Lagrenee, B. Mernari, F. Bentiss, *Corros. Sci.* 50 (2008) 473-479

[16] Mesbah, C. Juers, Lacouture, F. Mathieu, S. Rocca, E. Francois, J. Steinmetz, J. *Solid State. Sci* 9 (2007) 322-328

[17] N. Nagm, N.G. Kandile, E.A. Bad R, M.A. Mohammd, Corros. Sci 65 (2012) 94-103

[18] N.G. Thompson, M. Yunovich, D. Don mire, *Corrosion Rev.* 25 (2007) 247-262

[19] N.O. Eddy, B.I. Ita, S.N. Dodo, E.D. Paul, Green Chem. Lett. Rev. 5 (2012). 43 – 53.

[20] N.S. Patel, S. Jauhariand, G.N. Melita, S.S. Al-Deyeb, I. Warad, B. Hammouti, *Int. J. Electrochem. Sci.* 8 (2013) 2635-2655

[21] P.C. Okafor, V.I. Osabor, E.E. Ebenso, *Pig. Res. Technol.* 36 (2007) 299-305

[22] P.L. Cabot, F.A. Centellas, J.A. Garrido, E. Perez, H. Vidal, *Electrochem. Acta* 36 (1991) 179

[23] P.R. Bothi, M.G. Sethuraman, *Mater Lett.* 62 (2008) 113-116

[24] S. Rajendran, A.J. Amalraj, M.J. Joice, N. Anthony, D.C. Trevedi, M. Sundaravadivelu, *Corrs. Rev.* 22 (2004) 233-248

[25] S.A. Umoren, E.E. Ebenso, *Mater Chem. Phys.* 106 (2007) 393

[26] S.A.M. Refeay, A.E. Malak, A.M. Taha, F. Abdel-Fatah, H.T.M. *Int. J. Electrochm. Sci*. 3 (2008) 167-176

[27] S.K. Sharma, A. Mudhoo, G. Jain, E. Khamisa. *Green Chem. Lett. Rev.* 2 (2009) 47-51

[28] S.R. Taylor, B.D. Chambers, *Corros. Rev.* 25 (2007) 571-590

[29] X. Li, S. Deng, *Corrosion Science* 65 (2012) 299-308

[30] E. Rodriquez-clemente, J.G. Gonzalez-Rodriguez and M.G. Valladares-Cisneros, *Int. J. Electrochem. Sci.* 9 (2014) 5924-5936

[31] Espinoza-vazquez, G.E. Negron-Silva, D. Angeles-Beltran., H. Herrera-Hernandez, M. Romero-Romo, M. Palomar-Par dave. *Int. J. Electrochem. Sci.* 9 (2014) 493-509

[32] S. Abd El-Aziz Fouda, Ahmed Abdel Nazeer, Y. Ayman El-Khateeb, and Mohamed Fakih. *Journal of the Korean Chemical Society* 58 (2014) 359-365

[33] Krzysztof Rokosz, Tadeusz Hryniewicz. *World Scientific News* 35 (2016) 44-61

[34] Krzysztof Rokosz, Tadeusz Hryniewicz. *World Scientific News* 37 (2016) 232-248

[35] Krzysztof Rokosz, Tadeusz Hryniewicz, Patrick Chapon, Łukasz Dudek. *World Scientific News* 57 (2016) 289-299

[36] F. E. Abeng, V. D. Idim, O. E. Obono, T. O. Magu, *World Scientific News* 77(2) (2017) 298-313

[37] Krzysztof Rokosz, Tadeusz Hryniewicz, Kornel Pietrzak, Łukasz Dudek, Winfried Malorny. *World Scientific News* 70(2) (2017) 71-85